Provided for non-commercial research and education use.
Not for reproduction, distribution or commercial use.

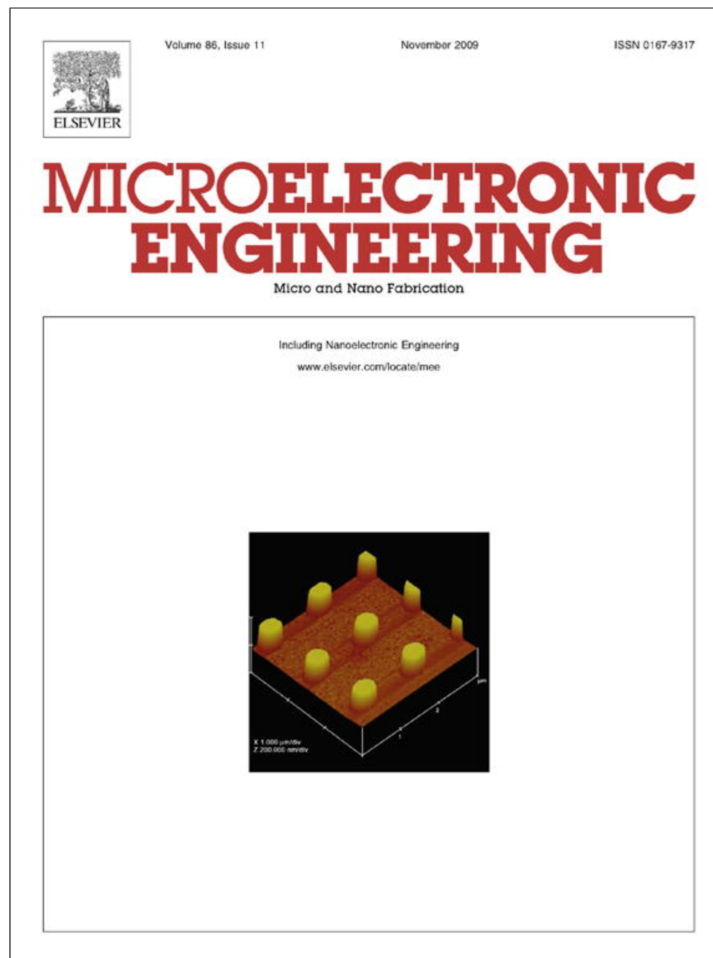


This article appeared in a journal published by Elsevier. The attached copy is furnished to the author for internal non-commercial research and education use, including for instruction at the authors institution and sharing with colleagues.

Other uses, including reproduction and distribution, or selling or licensing copies, or posting to personal, institutional or third party websites are prohibited.

In most cases authors are permitted to post their version of the article (e.g. in Word or Tex form) to their personal website or institutional repository. Authors requiring further information regarding Elsevier's archiving and manuscript policies are encouraged to visit:

http://www.elsevier.com/copyright

Author's personal copy

Microelectronic Engineering 86 (2009) 2364–2368

Contents lists available at ScienceDirect

Microelectronic Engineering

journal homepage: www.elsevier.com/locate/mee

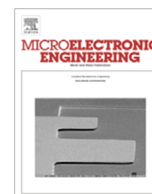

# Bimorph nano actuators synthesized by focused ion beam chemical vapor deposition

Jiyoung Chang [a], Byung-Kwon Min [b], Jongbaeg Kim [b,*], Liwei Lin [a]

[a] Berkeley Sensor and Actuator Center, University of California at Berkeley, CA, USA
[b] School of Mechanical Engineering, Yonsei University, 134 Shinchon-dong, Seodaemun-gu, Seoul, South Korea

ARTICLE INFO

*Article history:*
Received 19 November 2008
Received in revised form 18 March 2009
Accepted 21 April 2009
Available online 3 May 2009

*Keywords:*
Nano actuator
Bimorph
Focused ion beam
Chemical vapor deposition

ABSTRACT

Bimorph nano actuators synthesized by a two-layer focused ion beam (FIB) chemical vapor deposition (CVD) process have been demonstrated. The core bimorph segment of the actuator is a column structure made of two 200-nm thick tungsten-based-conductor (TBC) and diamond-like-carbon (DLC) layers. Several segments can be connected together of different angles to construct actuators with various moving capabilities when joule heating is applied via silicon MEMS (Microelectromechanical System) heater as the actuation source. Experimentally, a prototype five-segment actuator has shown projection displacement of 600 ± 60 nm under an input power of 1.02 W (160 mA and 6.41 V). The actuator has been repeatedly operated for over 100 times without any indication of degradation. As such, this work represents a new class of nano actuators based on versatile and flexible FIB-CVD bimorph nanostructures.
© 2009 Elsevier B.V. All rights reserved.

## 1. Introduction

Nano actuators capable of sub-micron manipulation could play an important role in the advancement of nanotechnologies. Previously, carbon nanotubes (CNT) have been demonstrated as the foundation of nano actuators using electrostatic force, such as single-electrode or double-electrode CNT-tweezers [1]. Several top-down fabrication processes by means of FIB-CVD have also been used to fabricate nano actuators. These include a three-dimensional nano rotor [2], tungsten and silicon dioxide-based bimorph [3] and a cell wall cutting tool [4]. Also, hybrid platinum/SWCNT actuators have been studied as metallic artificial muscles by modulating surface electronics charge density with respect to surrounding electrolyte [5]. On the other hand, researchers have reported different kinds of micro actuators fabricated by MEMS technologies, including electrostatically driven [6], electromagnetically driven [7], thermally driven [8] and bimorph-type micro actuators [9–12]. Among these, thermal actuators typically have advantages in easy actuation and fabrication such that we choose thermal actuation as the foundation in the design of nano actuators here. This work presents bimorph nano actuators by adopting the flexible fabrication capability of FIB-CVD [2–4,13] to construct bimorph nanostructures on top of MEMS heaters for functional demonstrations in nano actuation.

## 2. Design, fabrication and acutation

Fig. 1 shows the schematic view of the bimorph nano actuator sitting on top of a MEMS heater which functions as both the mechanical platform and joule heating source. Strategically, the nano actuator is placed at the center of the MEMS heater for maximum temperature inputs and is constructed in the out-of-plane direction for easy synthesis and observation. MEMS heaters are fabricated using a one-mask SOI (Silicon on Insulator) process similar to the process used to make micro vertical, torsional actuators [14,15] and scanning micro mirrors [6]. The sacrificial silicon dioxide layer has not been etched away in this case to prevent self-bulking of the MEMS heater [16] and preserve the movement of the nano actuator. Focused ion beam chemical vapor deposition (FIB-CVD) is applied to deposit the bimorph materials and construct the nano structure to have several bimorph segments as illustrated in the inset of Fig. 1. The length of each segment is set at 5 μm and thickness is 400 nm by depositing 200-nm thick tungsten-based-conductor using hexacarbonyl [$W(CO)_6$] as the CVD gas source followed by another 200-nm thick diamond-like-carbon deposition using phenanthrene vapor [$C_{14}H_{10}$] as the source material. The length, thickness and angle control is conducted using the SII3050 machine from SEIKO and several equipment- and material-related constraints result in the final choices of these parameters. Fabrication condition for bimorph nano actuator is tabulated in Table 1.

First, it is found that if $C_{14}H_{10}$ is used as the base structure instead of $W(CO)_6$, buckling occurs around the center of segment.

* Corresponding author. Tel.: +82 2 2123 2812.
*E-mail address:* kimjb@yonsei.ac.kr (J. Kim).

0167-9317/$ - see front matter © 2009 Elsevier B.V. All rights reserved.
doi:10.1016/j.mee.2009.04.022

Author's personal copy



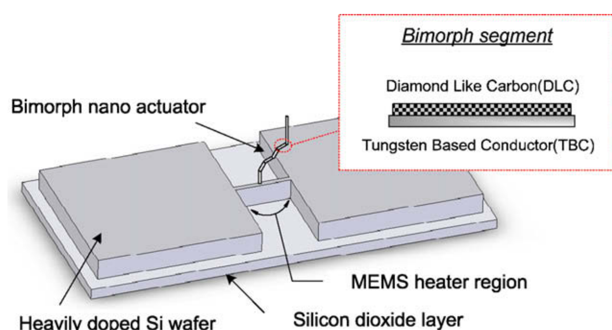


**Fig. 1.** Schematic view of the prototype, 5-segment, bimorph nano actuator. Joule heating on MEMS heater is the source of actuation. The silicon dioxide layer is sitting on top of a silicon substrate which is not drawn here. Inset shows a single bimorph segment that consists of both diamond-like-carbon (DLC) and tungsten-based-conductor (TBC) materials.

**Table 1**
Bimorph nano-actuator fabrication condition using FIB-CVD.

| Gas materials | Phenanthrene vapor ($C_{14}H_{10}$) | Tungsten Hexacarbonyl ($W(CO)_6$) |
|---|---|---|
| Beam current (pA) | 9.1 | 9.1 |
| Beam diameter (nm) | 13 | 13 |
| Dwell time (μs) | 0.5 | 0.5 |
| Spot irradiation deposition rate (μm/min) | ≈1 | ≈0.2 |

The reason is probably that carbon based structures cannot withstand the local stress generated during the tungsten based deposition in the FIB-CVD process. Therefore, TBC is chosen as the base structure and DLC is designated as the add-on structure in the core bimorph segment. Second, the deposition thickness in FIB-CVD is determined from the beam current used in the FIB-CVD system. While one can deposit structures with smaller thickness by lowering the beam current, uncertainty in dimensional control becomes problematic such that 200 nm is chosen as the standard deposition thickness in this work. Third, the length of each bimorph segments is chosen to be 5 μm considering overall dimensional accuracy of the structure and fabrication efficiency.

This versatile fabrication feature makes possible of various designs to amplify the actuation movement. In the prototype designs, five segments are placed in a plane normal to the MEMS chip and connected with either 30° or 60° angle between two successive segments while an identification pillar is added at the end as shown in Fig. 2a. Bimorph segments with connecting angles of 30° and 60° are chosen to show versatility of the process as well as possible controls for the movement at the end point of identification pillar. The multi-segment design as shown also reveals several other important aspects of the nano actuator. It is noted that TBC structures are connected continuously while DLC structures are not connected in neighboring segments. This design preserves the bending of individual bimorph segment to allow maximum bending movement while preventing the accumulation of strain in the joint region. In the process, the TBC structure in each segment has a design length of 5.2 μm and the DLC structure has a design length of 5 μm. However, in real fabrication conditions, control of these fine dimensions is difficult to achieve. For example, Fig. 2b and c are two photos from Scanning Ion Microscope (SIM) of two joint regions of the nano actuator. Several fabrication flaws can be easily identified, including the alignment problem of the TBC and DLC layers, fine dimensional control of the gap between two segments, overlapping of the ends of joints, possible variations in the tilt angle, and variations in cross section area of the nano actuator.

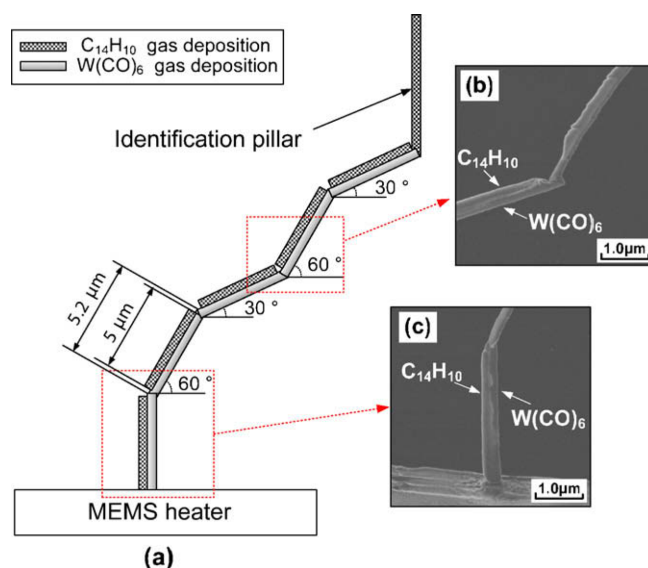


**Fig. 2.** (a) Side view of the nano actuator. The two SIM images in (b) and (c) show two different areas of the structure and relatively poor dimensional control of the manufacturing process.

Scanning Ion Microscope (SIM) image in Fig. 3a highlights the MEMS heater which is 100-μm long, 10-μm wide and 50-μm thick, *p*-type heavily doped silicon with resistivity of 0.02 Ω cm and Fig. 3b shows the fabricated bimorph nano actuator. The nano actuator is very small as compared to the MEMS actuator such that it is not observable in Fig. 3a. The dimension of the nano actuator is 13.6 μm in width and 23.7 μm in height as measured in Fig. 3b and both dimensions match relatively well with the theoretical design values.

The actuation measurement is performed in air under room temperature. DC voltage is applied to the MEMS heater via the two rectangular contact pads. In Fig. 4, *I–V* curve of MEMS heater and corresponding measured "projection displacement" of the bimorph nano actuator are plotted. The measured projection displacement is defined as the projected length observed from the top side of the MEMS heater as shown in Fig. 5a. Experimentally, the highest input voltage that can operate the nano actuator repeatedly is 0.16 A (6.41 V) and the projection displacement is 600 ± 60 nm as shown in Fig. 5. Experimental measurements are conducted under an optical microscope and later by overlapping four images together. The first two photos focus on the bottom of the actuator at point (C) such that it is visible as a small dot in the images with and without the electrical power input. The other two photos are taken by focusing on the tip of the identification pillar at point (A) and (B), respectively, before and after applying the electrical power input at 1.02 W. The projection displacement is measured by placing and aligning optical images in Microsoft Visio similar to that of Fig. 5 and draws parallel lines over the base and tip points of the actuator. The displacement is calculated based on the ruler distance as indicated in Fig. 5. The 60 nm uncertainty is estimated from this measurement scheme in which the size of each grid is 30 nm. This actuation has been conducted 100 times without signs of degradation or permanent deformation of the nanostructure. However, when the applied power went above 1.5 W, the nano actuator was not able to recover back to its original position. As noted before in the previous session, DLC can easily deform as compared with TBC when temperature rises. We suspect that this is the key reason for the permanent deformation. When the applied current went over 0.31 A, the MEMS structure was broken around the center region as the temperature can be high and close to the melting temperature of silicon. Fig. 4 also reveals that

Author's personal copy



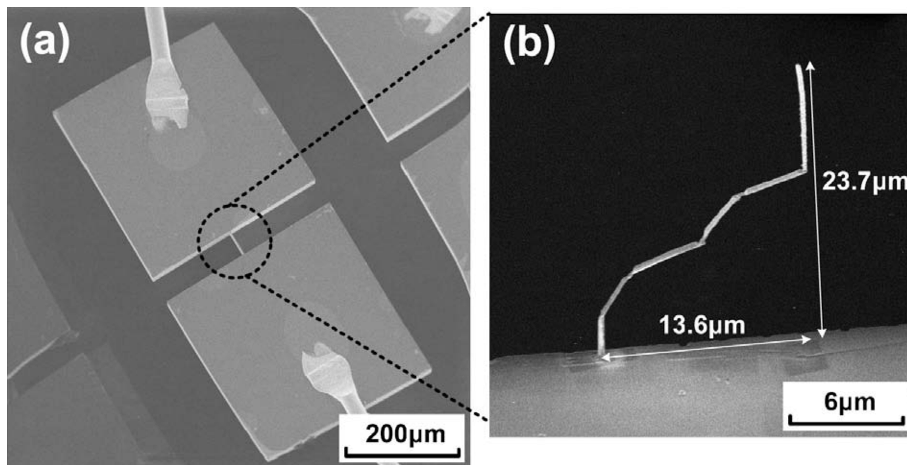


**Fig. 3.** (a) SIM image of micro heater that has been wire bonded. (b) SIM image of fabricated nano actuator with five, 5 μm-long bimorph segments and one 10 μm-long identification pillar at the tip.

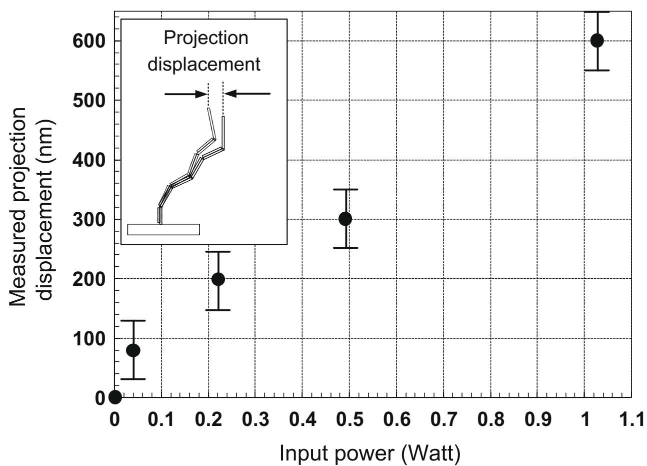


**Fig. 4.** Measured input power and corresponding projection displacement. The highest input power without causing permanent damage is 1.02 W and the corresponding projection displacement is about 600±60 nm.

the projection displacements generally follow the trend of the input power in this repeatable operation region.

## 3. Analyses and discussion

Since the suggested bimorph nano actuator is composed of several bimorph segments, the coefficient of thermal expansion (CTE) mismatch ($\Delta\alpha$ is the key factor in deciding its performance. First-order approximations can be conducted to analyze the structure based on several simplified assumptions: (1) the cross section of the segment is rectangular, (2) the temperature of the bimorph is uniform within the whole structure and is the same as that at the center of the MEMS heater. The analysis starts with one bimorph segment using the D–H (Denavit–Hartenberg) method. The Young's modulus of $C_{14}H_{10}$ and $W(CO)_6$ based materials are estimated as 100 GPa [17] and 300 GPa [18], respectively. The angle change in each segment ($\theta$) as illustrated in Fig. 6a can be expressed in terms of difference of CTE ($\Delta\alpha$) of the two materials and temperature rise ($\Delta T$) [19] as well as parameters including the bimorph structural dimensions and Young's modulus of each layer. The projection displacement at the tip of the identification pillar is the combination of the movement of all bimorph segments as shown in Fig. 6b. The temperature change of the MEMS heater is estimated by an electric-thermal FEM analysis [20,21]. Fig. 6c shows that the hottest spot of the MEMS heater is the center portion of the microbridge where the nano bimorph is constructed and

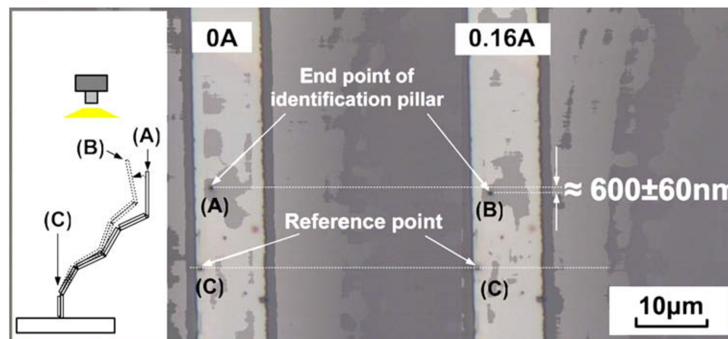


**Fig. 5.** Synthesized optical image for the measurement of the projection displacement. This image is the fusion of four optical photos. The focuses of the first two photos are on the bottom of the actuator to show point (c) as a visible dot in this synthesized image, representing conditions before and after applying the electrical power. The other two photos are taken by focusing on the tip of the identification pillar at points (A) and (B), respectively, representing lateral displacements before and after applying the electrical power at 1.02 W, respectively.

Author's personal copy



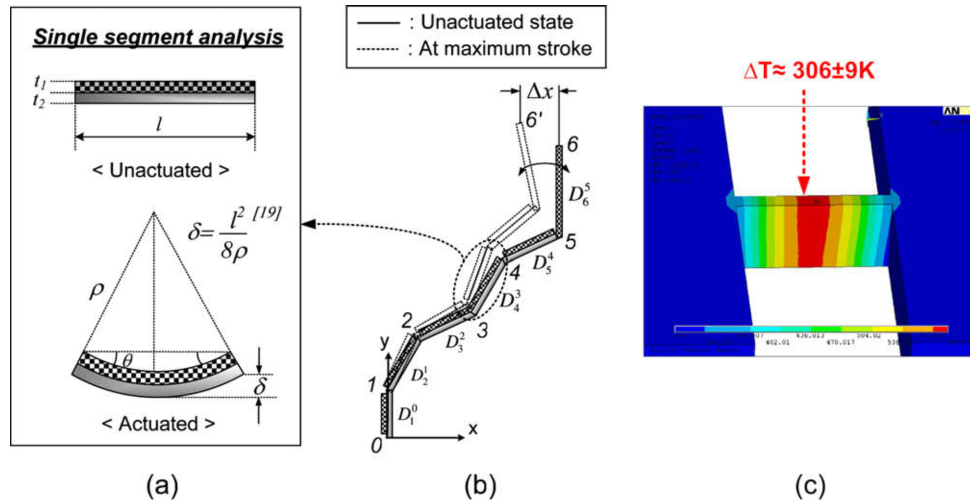


**Fig. 6.** (a) D-H method is used to estimate the actuation displacement. (b) Projection displacement ($\Delta x$) is the combination movements of all bimorph segments. (c) FEM simulation showing that highest temperature increment ($\Delta T$) at the center of the MEMS heater without causing permanent damages is 306±9 K under 1.02 W (0.16 A, 6.41 V).

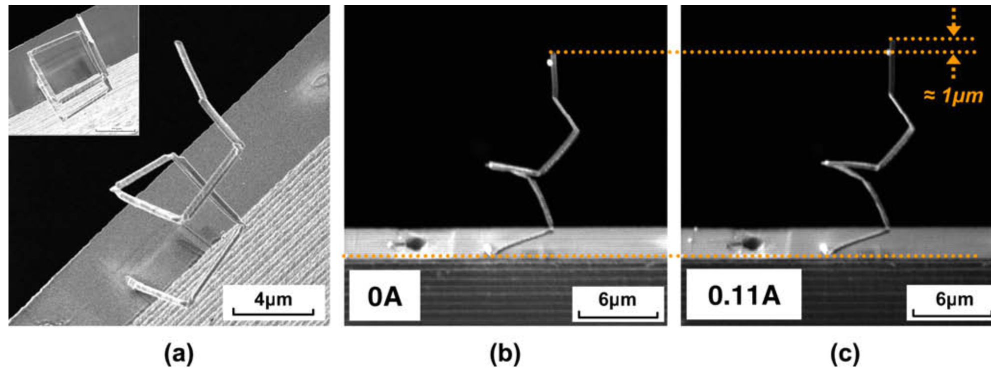


**Fig. 7.** (a) A spiral-shape bimorph nano actuator consisting of seven segments and one identification pillar to achieve straight vertical movements. Inset is from another viewing angle. (b) and (c) Side view images in the FIB chamber before and after applying 0.11 A input power. An upward displacement of 1 μm from the nano actuator is estimated.

the maximum temperature rise of 306 ± 9 K is obtained. In this simulation, convection is neglected. The radiation is also ignored due to its small size compared to the MEMS structure and large angle between adjacent segments. These information and analysis can lead to several conclusions. First, TBC has higher CTE such that the bimorph segment is bending concavely when TBC is the bottom layer and temperature is heating up. Second, the CTE mismatch, $\Delta\alpha$, between TBC and DLC is estimated at $1.9 \times 10^{-6}\,K^{-1}$ based on this first order analysis by fittings with simulation and experimental results.

The aforementioned bimorph nano actuator is constructed in a plane normal to the ground plane and is capable of making arc-shape movement due to the bending of bimorph segments. Theoretically, it is possible to achieve "straight vertical movement" with special designs. For example, inspired by spiral spring shape, we designed and fabricated a seven-segment bimorph nano actuator that has the theoretical moving direction normal to the ground plane as shown in Fig. 7a. The final portion of the structure is an identification pillar made of TBC. The inset SIM image shows another view of the structure to illustrate the spiral-shape design as each of the consecutive bimorph segment is turned by 90° (counterclockwise viewing from the top) in the lateral direction and 30° upwards in the vertical direction with respect to the ground plane. The actuation is observed in the FIB vacuum chamber by connecting electrical connections into the chamber to monitor sub-micron movements. It is observed that before and after the application of 0.11 A (4.9 V) in Fig. 7b and c, respectively, the nano actuator moves upward about 1 μm. Several issues have contributed to possible large uncertainly of this measurement. First, the control issues and fabrication variations in FIB-CVD can cause significant deviations from the preferred design values such that the fabricated device does not necessarily match the design specifications. Second, the SIM images should be perpendicular to the ground plane to minimize measurement errors. As both issues are difficult to resolve in this prototype demonstration, lateral motion in addition to vertical motion is expected in the measurements of this prototype device.

Relatively high power input for the achieved displacement is attributed to the excessively large MEMS heater used. By designing smaller heater on a thinner layer instead of 50 μm thick SOI, the input power is expected to be substantially decreased generating similar level of temperature.

## 4. Conclusion

Bimorph nano actuators have been successfully fabricated using FIB-CVD deposition with versatile design and material choices based on core bimorph segments made of TBC and DLC nanostruc-

Author's personal copy



tures. The measured projection displacement in a prototype, five-segment structure is 600 ± 60 nm under joule heating by input power of 0.16 A (6.41 V) to a 100-μm long, 10-μm wide and 50-μm thick MEMS heater. The actuation has been operated repeatedly for 100 times without noticeable degradation of the nanostructure. First-order analysis is conducted to characterize and establish the relationships between applied current, temperature, geometry and mechanical properties of the nano actuator. A spiral-shape design is experimented in order to achieve straight, vertical displacement at the tip of the nano actuator. Although experimental results do not exactly match the theoretical prediction due to fabrication deviations and other factors, this work provides design guidelines and examples on the versatility in motion capability of nano actuators based on bimorph segments.

## Acknowledgements

This work was supported by the Korea Research Foundation Grant funded by the Korean Government (MOEHRD, Basic Research Promotion Fund) (KRF-2006-311-D00024) and Nano R&D program through the Korea Science and Engineering Foundation funded by the Ministry of Education, Science and Technology (2008-02916).

## References

[1] P. Kim, C.M. Lieber, Science 286 (1999) 2148–2150.
[2] J.-y. Igaki, R. Kometani, K.-i. Nakamatsu, K. Kanda, Y. Haruyama, Y. Ochiai, J.-i. Fujita, T. Kaito, S. Matsui, Microelectronic Engineering 83 (2006) 1221–1224.
[3] C. Minari, R. Kometani, K. Kanda, Y. Haruyama, T. Kaito, S. Matsui, W/$SiO_2$ thermal bimorph nano-actuator fabrication by focused-ion-beam chemical-vapor-deposition, in: Abstract of the 50th International Conference on Electron, Ion, and Photon Beam Technology and nanofabrication, Baltimore, Maryland, May 30–June 2, 2006, pp.193–194.
[4] R. Kometani, R. Funabiki, T. Hoshino, K. Kanda, Y. Haruyama, T. Kaito, J.-i.. Fujita, Y. Ochiai, S. Matsui, Microelectronic Engineering 83 (2006) 1642–1645.
[5] S. Lu, B. Panchapakesan, Nanotechnology 17 (2006) 888–894.
[6] J. Kim, C. Dane, L. Lin, Photonics Technology Letters, IEEE 17 (2005) 2307–2309.
[7] A. Cao, J. Kim, L. Lin, Journal of Micromechanics and Microengineering 17 (2007) 975–982.
[8] L. Lin, S.-H. Lin, Sensors and Actuators A: Physical 71 (1998) 35–39.
[9] H. Sehr, A.G.R. Evans, A. Brunnschweiler, G.J. Ensell, T.E.G. Niblock, Journal of Micromechanics and Microengineering 11 (2001) 306–310.
[10] J. Teng, P.D. Prewett, Sensors and Actuators A: Physical 123–124 (2005) 608–613.
[11] L. Zhihua, W. Yangjie, C. Ho-Yin, L. Wen Jung, D. Zaili, W. Yuechao, Structural and thermal analysis of a thermally actuated polymer micro robotic gripper, in: IEEE ROBIO, 2004, pp. 470–473.
[12] H. Sehr, I.S. Tomlin, B. Huang, S.P. Beeby, A.G.R. Evans, A. Brunnschweiler, G.J. Ensell, C.G.J. Schabmueller, T.E.G. Niblock, Journal of Micromechanics and Microengineering 12 (2002) 410–413.
[13] J. Chang, J. Kim, B.-K. Min, S. J. Lee, L. Lin, Electrostatically actuated nano tweezers fabricated on micro processed electrodes, in: First IEEE NEMS Zhuhai, China, 2006, pp. 1440–1444.
[14] J. Kim, D. Christensen, L. Lin, Sensors and Actuators A: Physical 127 (2006) 248–254.
[15] J. Kim, H. Choo, L. Lin, R.S.A.M.R.S. Muller, Journal of Microelectromechanical Systems 15 (2006) 553–562.
[16] M. Chiao, L. Lin, Journal of Microelectromechanical Systems 9 (2000) 146–151.
[17] M. Ishida, J.-i.. Fujita, Y. Ochiai, Journal of Vacuum Science & Technology B 20 (2002) 2784–2787.
[18] M. Ishida, J. Fujita, T. Ichihashi, Y. Ochiai, T. Kaito, S. Matsui, Journal of Vacuum Science & Technology B 21 (2003) 2728–2731.
[19] S. Timoshenko, Journal of the Optical Society of America 11 (1925) 233–256.
[20] A.F. Mills, Basic Heat and Mass Transfer, second ed., Prentice Hall, Upper Saddle River, NJ, 1999.
[21] L. Lin, M. Chiao, Sensors and Actuators A: Physical 55 (1996) 35–41.